ChemPubSoc Europe

DOI: 10.1002/cbic.201800399

CHEMBIOCHEM Full Papers

Cyano Modification on Uridine Decreases Base-Pairing Stability and Specificity through Neighboring Disruption in RNA Duplex

Song Mao,[a] Srivathsan V. Ranganathan,[a] Hsu-Chun Tsai,[a] Phensinee Haruehanroengra,[a] Fusheng Shen,[a] Vibhav A. Valsangkar,[a] Bo Han,[a, b] Abdalla E. A. Hassan,[c] Alan Chen,[a] and Jia Sheng*[a]

5-Cyanomethyluridine (cnm^5U) and 5-cyanouridine (cn^5U), the two uridine analogues, were synthesized and incorporated into RNA oligonucleotides. Base-pairing stability and specificity studies in RNA duplexes indicated that cnm^5U slightly decreased the stability of the duplex but retained the base-pairing preference. In contrast, cn^5U dramatically decreased both base-pairing stability and specificity between U:A and other noncanonical U:G, U:U, and U:C pairs. In addition, the cn^5U:G pair was found to be stronger than the cn^5U:A pair and the other mismatched pairs in the context of a RNA duplex; this implied that cn^5U might slightly prefer to recognize G over A. Our mechanistic studies by molecular simulations showed that the cn^5U modification did not directly affect the base pairing of the parent nucleotide; instead, it weakened the neighboring base pair in the 5′ side of the modification in the RNA duplexes. Consistent with the simulation data, replacing the Watson–Crick A:U pair to a mismatched C:U pair in the 5′-neighboring site did not affect the overall stability of the duplex. Our work reveals the significance of the electron-withdrawing cyano group in natural tRNA systems and provides two novel building blocks for constructing RNA-based therapeutics.

Introduction

RNA plays essential and diverse roles in living systems as a genetic information carrier, functional regulator, and catalyst.[1–4] The structures and functions of RNA in cells are further diversified in the presence of various post-transcriptional chemical modifications. To date, more than 150 chemical modifications that decorate different positions of nucleobases and ribose in RNA nucleotides have been discovered in all the natural life domains.[5–7] These chemical modifications are able to mediate and fine-tune many specific base-pairing patterns,[8] which are critical for RNA to fold into well-defined functional structures. Therefore, understanding fundamental base-pairing stability and specificity provides a foundation for elucidating RNA structure–function relationships and for engineering novel RNA-based therapeutics.[9]

Transfer RNA (tRNA), the adaptor molecule linking the codons of messenger RNA to the corresponding amino acids during protein synthesis, contains more than 100 chemical modifications that are post-transcriptionally introduced by specific enzymes.[5] In particular, the "wobble" position 34 of a tRNA, the first anticodon letter, is usually modified by a wide variety of chemical groups for stable structural maintenance, efficient decoding capabilities, and accurate amino acid recognition/integration by the translation machinery.[10–15] 5-Cyanomethyluridine (cnm^5U) was recently discovered as a new naturally modified nucleoside at the wobble position of isoleucine

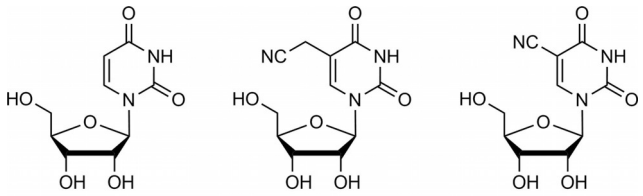

tRNAs from mutant *Haloarcula marismortui*.[16] In addition, cnm^5U is present in the total tRNA of *Methanococcus maripaludis*, which is indicative of its widespread occurrence in Euryarchaea tRNAs.[16] This mutant tRNA binds not only to AUA

[a] Dr. S. Mao, Dr. S. V. Ranganathan, H.-C. Tsai, P. Haruehanroengra, F. Shen, V. A. Valsangkar, Prof. B. Han, Prof. A. Chen, Prof. J. Sheng
Department of Chemistry and The RNA Institute
University at Albany, State University of New York
1400 Washington Avenue, Albany, NY, 12222 (USA)
E-mail: jsheng@albany.edu

[b] Prof. B. Han
School of Pharmacy, Chengdu University of Traditional Chinese Medicine
Chengdu, 611137 (China)

[c] Prof. A. E. A. Hassan
Applied Nucleic Acids Research Center
Faculty of Science, Zagazig University
Zagazig (Egypt)

Supporting Information and the ORCID identification numbers for the authors of this article can be found under https://doi.org/10.1002/cbic.201800399.

but also to AUU, another isoleucine codon, and to AUG, a methionine codon, which results in the nonspecific replacement of isoleucine by methionine during protein expression.[16] This mixed codon recognition pattern implies low base-pairing specificity of this cnm^{5}U residue in RNAs.

Toward our goal of studying detailed working mechanisms of naturally modified RNA nucleotides, we report here the new synthesis of cnm^{5}U-containing RNA oligonucleotides and their base-pairing stability and specificity studies in the context of RNA duplexes. In addition, many naturally and artificially modified nucleotides have been widely used in developing DNA/RNA-oligonucleotide-based therapeutics through antisense or RNAi strategies.[17] The introduction of these modified residues can increase strand stability, facilitate their cellular delivery/transportation, and improve their targeting specificity and efficiency. Therefore, inspired by naturally occurring cnm^{5}U, we also synthesized 5-cyanouridine (cn^{5}U), a close analogue of cnm^{5}U with the electron-withdrawing cyano group directly attached to uracil, and RNA strands containing this modification. Comparison of the base-pairing stability and specificity in the same RNA duplex indicated that cnm^{5}U slightly decreased duplex stability but retained the base-pairing preference with native U. In contrast, cn^{5}U dramatically decreased base-pairing stability and specificity between cn^{5}U:A and other noncanonical cn^{5}U:G, cn^{5}U:U, and cn^{5}U:C pairs. Subsequent mechanistic studies by molecular simulations showed that the cn^{5}U modification did not directly affect the base pairing of the parent nucleotide; instead, it weakened the neighboring base pair in the 5′ side of the modification in the RNA duplexes. Consistent with the simulation data, replacing the Watson–Crick A:U pair to a mismatched C:U pair in the 5′-neighboring site did not affect the overall stability of the duplex. Our work reveals the significance of the electron-withdrawing cyano group in natural tRNA systems and provides two novel building blocks for constructing RNA-based therapeutics.

Results and Discussion

Chemical synthesis of the cnm^{5}U and cn^{5}U phosphoramidite building blocks and their RNA oligonucleotides

Although the synthesis of the cnm^{5}U and cn^{5}U nucleosides was previously achieved,[18–21] more general phosphoramidite building blocks for the solid-phase synthesis of oligonucleotides are still required to make different scales of RNA strands. We started the synthesis of cnm^{5}U from commercially available 5-methyluridine (**1**, Scheme 1), which was fully acetyl protected; this was followed by bromination of the 5-methyl group in the presence of *N*-bromosuccinimide (NBS) and 2,2′-azobisisobutyronitrile (AIBN) to give 5-bromomethyluridine (**3**). The cyano group was subsequently installed by treatment with TMSCN and tetrabutylammonium fluoride (TBAF), which was followed by deprotection of the acetyl groups by using ammonia to yield 5-cyanomethyluridine (**5**). The 5′- and 2′-hydroxy groups were selectively protected with dimethoxyltrityl (DMTr) and *tert*-butyldimethylsilyl (TBDMS) groups, respectively, to obtain 2′,5′-protected cnm^{5}U compound **7**, which is the key intermediate to make final phosphoramidite building block **8** for the solid-phase synthesis of the oligonucleotides.

The synthesis of 5-cyanouridine began with regular Vorbrüggen glycosylation of the protected ribofuranose with silylated 5-cyanouracil **10** (Scheme 2) in the presence of tin(IV) chloride, and this was followed by deprotection of the benzoyl (Bz) groups by base treatment. Simultaneous silylation of the 3′- and 5′-hydroxy groups with di-*tert*-butylsilyl ditriflate followed by 2′-protection with a TBDMS group gave silylated 5-cyanouridine **13**. Subsequently, this compound was selectively desilylated by using hydrogen fluoride in pyridine (HF·Py) and was then tritylated with trityl chloride at the 5′-position to generate key intermediate **15**, which was converted into final cn^{5}U

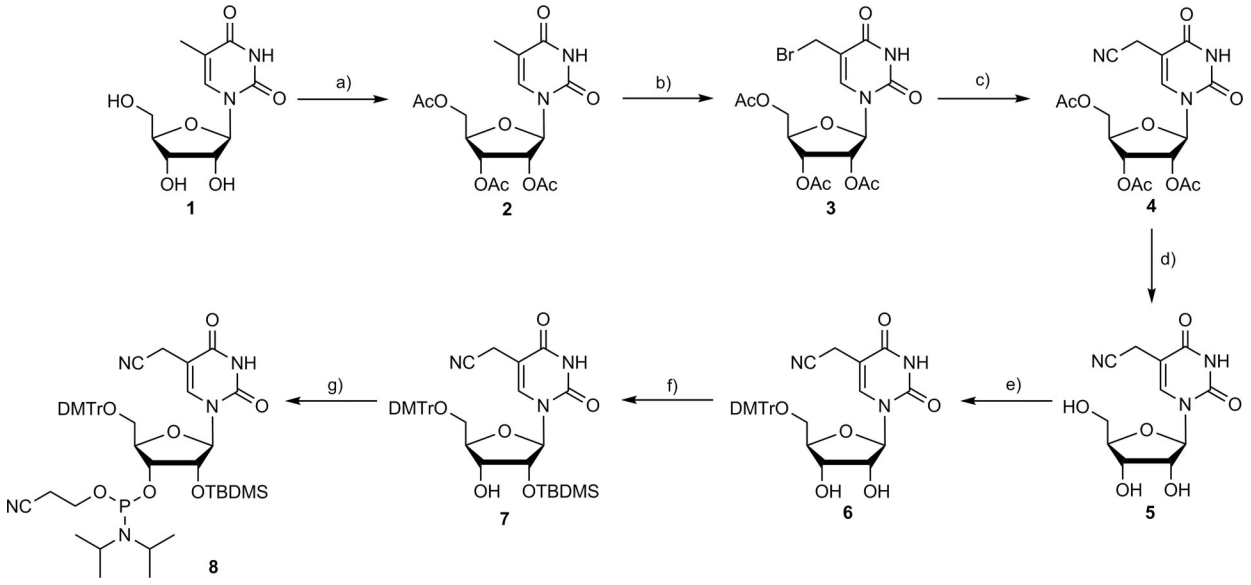

Scheme 1. Synthesis of 5-cyanomethyluridine phosphoramidite **8**. a) Ac_2O, DMAP, pyridine; b) NBS, AIBN, benzene; c) TMSCN, TBAF, THF; d) NH_3, MeOH; e) DMTrCl, DMAP, pyridine; f) TBDMSCl, $AgNO_3$, pyridine, THF; g) $(iPr_2N)P(Cl)OCH_2CH_2CN$, $(iPr)_2NEt$, THF.

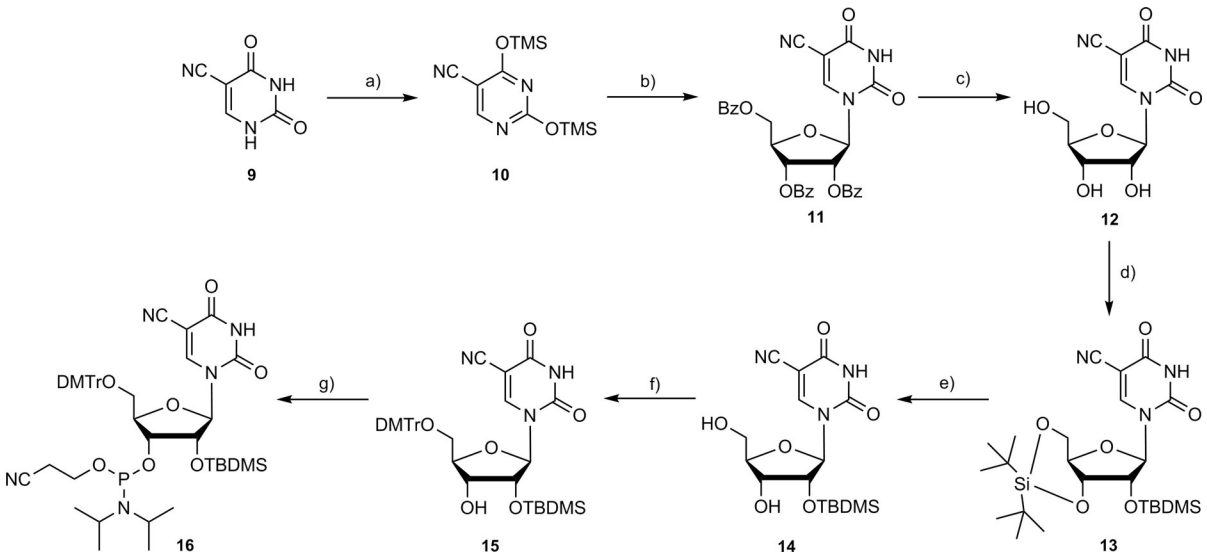

Scheme 2. Synthesis of 5-cyanouridine phosphoramidite **16**. a) TMSCl, HMDS; b) 2,3,5-tri-*O*-benzoyl-β-D-ribofuranose, $SnCl_4$, 1,2-dichloroethane; c) NH_3 in methanol; d) di-*tert*-butylsilyl ditriflate; TBDMSCl, imidazole, DMF; e) HF·Py, THF; f) DMTrCl, pyridine; g) $(iPr_2N)P(Cl)OCH_2CH_2CN$, $(iPr)_2NEt$, CH_2Cl_2.

phosphoramidite **16** through a regular phosphitylation reaction for the solid-phase synthesis.

As expected, both of the phosphoramidite building blocks were found to be well compatible with solid-phase synthesis conditions, including trichloroacetic acid (TCA) and oxidative iodine treatments, and thus, the coupling yields were very similar to those of the commercially available native phosphoramidites. They were also found to be stable to basic cleavage from the solid-phase beads and $Et_3N{\cdot}3\,HF$ treatment to remove the TBDMS groups during deprotection and purification of the RNA oligonucleotide. As a demonstration, nine different RNA sequences containing these two modifications were synthesized, and their structures were confirmed by ESI or MALDI MS, as shown in Table 1.

Thermal denaturation and base-pairing studies of the cnm^{5}U and cn^{5}U RNA duplexes

With these RNA strands in hand, we studied the base-pairing stability and specificity of both cnm^{5}U and cn^{5}U in RNA duplexes through UV–thermal denaturation experiments. The normalized melting temperature (T_m) curves of the native and modified RNA duplexes, [5′-GGACU**X**CUGCAG-3′ and 3′-CCUGA**Y**GACGUC-5′], with Watson–Crick and other noncanonical base pairs (X pairs with Y) are shown in Figure S40 in the Supporting Information. The detailed temperature data are summarized in Table 2. Compared to the native counterparts, the cnm^{5}U- and cn^{5}U-modified RNA duplexes both showed decreased thermal stability. In the normal U:A paired duplexes (Table 2, compare entries 1, 5, and 9), cnm^{5}U decreased T_m by 3.9 °C, whereas cn^{5}U dramatically decreased T_m by 20.7 °C; these values correspond to decreases in ΔG° of 4.8 and 7.8 kcal mol^{-1}, respectively. Similarly, the noncanonical base paired (U:G, U:C, and U:U) duplexes containing these two modifications also showed significantly lower melting temperatures. With cnm^{5}U, the T_m values dropped by 5.3 °C in the U:G mismatched duplex (Table 2, entry 2 vs. 6), by 3.0 °C in the U:C

Table 1. RNA sequences containing cnm^{5}U and cn^{5}U.

	RNA sequence	Mass [g mol^{-1}] calcd	found
ON1	AAUGCcnm^{5}UGCACUG	3832.55	3832.57
ON2	GGACUcnm^{5}UCUGCAG	3848.55	3848.56
ON3	UAGCcnm^{5}UCC	2178.33	2178.02
ON4	UCGcnm^{5}UACGA	2547.39	2547.13
ON5	Gcnm^{5}UACGUAC	2547.39	2547.40
ON6	AAUGCcn^{5}UGCACUG	3818.54	3819.14
ON7	GGACUcn^{5}UCUGCAG	3834.53	3834.54
ON8	UAGCcn^{5}UCC	2164.31	3164.32
ON9	UCGcn^{5}UACGA	2533.37	2533.38

Table 2. Duplex stability and base-pairing specificity of cnm^{5}U and cn^{5}U in a 12-mer RNA duplex.

		5′-GGACUXCUGCAG-3′ / 3′-CCUGAYGACGUC-5′			
	Base pair X→Y		T_m[a] [°C]	ΔT_m[b] [°C]	$-\Delta G^\circ_{37}$[c] [kcal mol^{-1}]
1	U	A	62.5		16.6
2	U	G	59.6	−2.9	16.0
3	U	C	50.9	−11.6	12.6
4	U	U	53.3	−9.2	14.0
5	cnm^{5}U	A	58.6		11.8
6	cnm^{5}U	G	54.3	−4.3	12.0
7	cnm^{5}U	C	47.9	−10.7	11.0
8	cnm^{5}U	U	49.1	−9.5	11.3
9	cn^{5}U	A	41.8		8.8
10	cn^{5}U	G	43.2	+1.4	9.0
11	cn^{5}U	C	39.8	−2.0	8.5
12	cn^{5}U	U	38.0	−3.8	8.1

[a] Measured in sodium phosphate (10 mM, pH 7.0) buffer containing 100 mM NaCl. [b] Relative to the RNA duplexes with the native and 5-modified U:A pair, respectively. [c] Obtained by nonlinear curve fitting by using Meltwin 3.5.[35]

mismatched one (Table 2, entry 3 vs. 7), and by 4.2 °C in the U:U mismatched one (Table 2, entry 4 vs. 8); these values correspond to decreases in ΔG° of 4.0, 1.6, and 2.7 kcal mol^{-1}, respectively. In the case of the cn^{5}U residue, for which the cyano group is directly attached to the uracil ring, the T_m values dropped by 16.4 °C in the U:G mismatched duplex (Table 2, entry 2 vs. 10), by 11.1 °C in the U:C mismatched one (Table 2, entry 3 vs. 11), and by 15.3 °C in the U:U mismatched one (Table 2, entry 4 vs. 12); these values correspond to decreases in ΔG° of 7.0, 4.1, and 5.9 kcal mol^{-1}, respectively. These results indicate that the cyano group on the 5-position of uracil has a strong effect on the overall base-pairing stability in the context of the RNA duplex such that a stronger electron-withdrawing effect to the uracil ring results in lower base-pairing stability.

On the other hand, comparison of the base-pairing specificity in each duplex system indicated opposite effects of these two modifications. Upon direct comparison of the T_m values of each Watson–Crick base-paired duplex with its own mismatched ones, as shown in the ΔT_m column of Table 2, cnm^{5}U retains base-pairing specificity that is similar to that of native U with slightly increased discrimination between the U:A and U:G pairs by 1.4 °C (Table 2, entry 2 vs. 6). However, cn^{5}U tends to decrease the base-pairing discrimination and makes the T_m differences much smaller than the native counterparts. For example, the T_m value of the cn^{5}U:C duplex is only 2 °C lower than that of the cn^{5}U:A paired one (Table 2, entry 9 vs. 11), compared to the native T_m difference of 11.6 °C. More interestingly, cn^{5}U changes the base-pairing preference and favors G over A by 1.4 °C, which corresponds to a ΔG° value of 0.2 kcal mol^{-1} (Table 2, entry 9 vs. 10).

Molecular simulation of cn^{5}U-modified RNA duplexes

To further explore the role of the cn^{5}U modification on lowering the base-pairing stability and specificity of RNA duplexes, we performed molecular dynamics (MD) simulations of the duplex in the presence and absence of the modification. Briefly, as outlined in the Experimental Section, we collected almost a microsecond of simulation data for both duplexes and analyzed the trajectories for differences in base-pairing propensities of the nucleotides. We calculated and compared the hydrogen-bonding distances (r_{NN}) between paired nucleotides (A/G-N1:U/C-N3, Figure 1 A). The time-series of r_{NN} for the modified cn5U6:A7 base pair is shown in Figure 1 C and that for a neighboring U5:A8 pair is shown in Figure 1 B. Interestingly, the behavior of r_{NN} for the cn^{5}U6:A7 base pair is unaffected by the presence of the modification, which indicates that the cyano modification does not directly affect the base-pairing propensity of the parent nucleotide. In contrast, we observed a significant difference in the hydrogen-bonding distances of the neighboring U5:A8 base pair. In the unmodified duplex, this UA base pair is largely in the paired state, and rare fraying events lead to an "open" state that is short lived (red lines in Figure 1 B). However, in the modified duplex, the fraying events occur much more often, along with a significant increase in the lifetimes of the open state (red lines in Figure 1 B). The time series r_{NN} data was converted into histograms, which are presented in Figure 1 D, E. The base-paired or "closed" states produce a strong band at approximately 3 Å for both sets of base-pairing nucleotides under consideration. However, the open states in the neighboring U5:A8 pair produces a weak second band in the histogram at approximately 5 Å (seen only in Figure 1 D, prominently in the log scale). Importantly, the prominence of the second band is approximately two orders of magnitude greater for the modified duplex than for the unmodified duplex, and this confirms a significant increase in the propensity of the neighboring AU base pair to

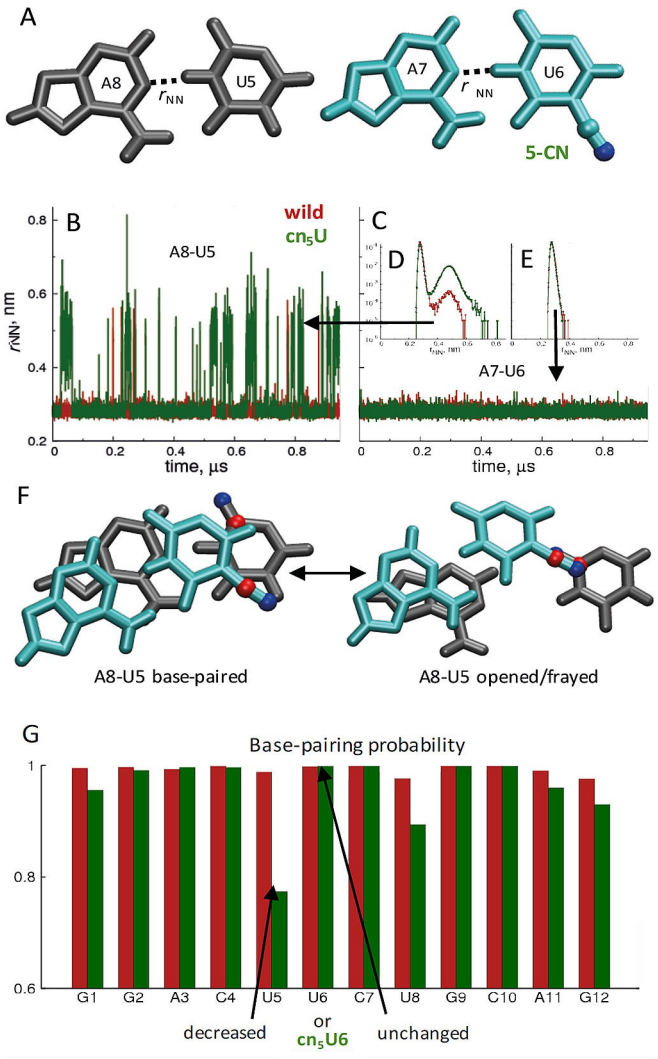

Figure 1. MD simulation results for the RNA duplex [5′-GGACUXCUGCAG-3′ & 3′-CCUGAYGACGUC-5′], for which X represents either modified or native U6 and Y represents the complimentary base A7. Nucleotide numbering is from the 5′-end in both strands. A) Base-pairing schemes for modified and unmodified A:U bases. Licorice representation was used for the bases, with the modification highlighted in CPK. B), C) Time series data, r_{NN} for the A8:U5 and A7:U6 base pairs, respectively. Unmodified duplex (wild) is shown in red, and the modified duplex is shown in green. D), E) Histograms for the time series data in (B) and (C), respectively. F) Simulation snapshots showing the dipole alignment of the modification in the open state. Same color coding as in panel A, except for the two dipoles, highlighted in red and blue. G) Base-pairing probabilities for the entire duplex (red: wild, green: modified).

adopt an open conformation in the presence of the modification.

The stacking view of two base-pairing steps (cn^{5}U6:A7 and U5:A8 in Figure 1F) with both open and closed states shows more detailed insight into the effect of this cyano modification on weakening the neighboring base pairing. The cyano modification can be regarded as a dipole, with roughly equal and opposite charges on the carbon and nitrogen atoms (colored in red and blue, respectively). In the open state, the C2–O2 bond of U5, which can also be treated as a dipole, perfectly aligns with the cyano group, which thereby stabilizes and favors the adoption of the open state; this in turn disrupts the local structures and might also allow higher hydration of the duplex, which therefore leads to lower stability of the overall duplex. In addition, this structural perturbation also decreases the specificity of the cn^{5}U6 pairing partners in terms of their contribution to the overall stability of the duplex.

We further extended the analysis to all the base pairs in this duplex, as presented in Figure 1G. We defined a cut off of $r_{NN} = 3.2$ Å to qualify base pairing and compared the unmodified (wild) and modified duplexes. It turned out that the modified duplex was overall unaffected by the presence of the modification (including the modified U6:A7 base pair), except for the weakening of the U5:A8 base pair.

To test if the weakening of the base pair on the 5′-neighbor of the modification site contributed towards lowering the overall duplex stability, we mutated the A8 residue to C in the complementary strand. As the base pairing is already weakened for this position, the mismatch mutation should not cause a significant change in the stability of the duplex. The thermal denaturation experiments of this mutated duplex (A8:U5 to C8:U5) showed very similar T_m values. However, mutating the 3′-end of the C:G pair decreased the overall stability of the duplex by 4.3 °C (Figure 2 and Table S2), which is consistent with our MD simulation results.

Conclusion

In summary, we synthesized cnm^{5}U and cn^{5}U phosphoramidites and a series of RNA oligonucleotides containing these two residues. Our base-pairing stability and specificity studies showed that the 5-cyano group on the uracil had strong effects on its base-pairing stability. Whereas the base-pairing specificity between U:A and other noncanonical pairs of cnm^{5}U was similar to that of native uridine, cn^{5}U dramatically decreased the discrimination between these base pairs. More interestingly, the cn^{5}U:G pair showed higher thermal stability than the cn^{5}U:A pair in the context of the RNA duplex, which implied that cn^{5}U might slightly prefer to recognize G over A. The molecular simulation studies results showed that the cn^{5}U modification did not directly affect the base pairing of the parent nucleotide; instead, it weakened the neighboring base pair in the 5′ side of the modification in the RNA duplexes. Consistent with the simulation results, replacing the Watson–Crick A:U pair to a mismatched C:U pair in the 5′-neighboring site did not affect the overall stability of the duplex. Although it has not been discovered in natural RNA systems, our results indicate that the cn^{5}U residue might be used by certain biological systems such as virus RNA to increase base-pairing diversify and to induce higher rates of gene mutation, even though it decreases the overall base-pairing stability. In addition, this work provides two novel building blocks for constructing RNA-based therapeutics.

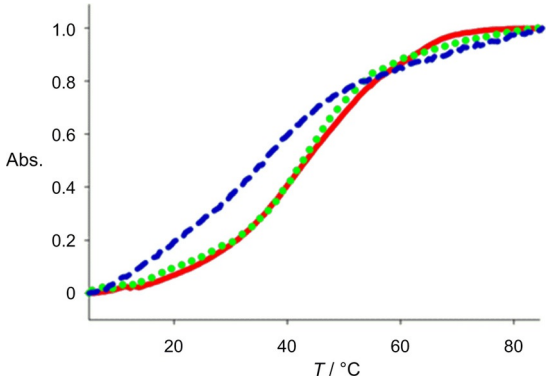

Figure 2. Normalized UV-melting curves of controlled RNA duplexes. The cn^{5}U-modified 5′-GGACU**cn^{5}U**CUGCAG-3′ sequence pairs with the 3′-CCU GA**A** GAC GUC-5′ strand (——), with the 3′-CCU GC**A** GAC GUC-5′ strand (····) and with the 3′-CCU GA**A** CAC GUC-5′ strand (-----).

Experimental Section

Materials and general procedures of synthesis: Anhydrous solvents were used and redistilled by using standard procedures. All solid reagents were dried under a high vacuum line prior to use. Air-sensitive reactions were performed under argon. RNase-free water, tips, and tubes were used for RNA purification, crystallization, and thermodynamic studies. Analytical TLC plates precoated with silica gel F254 (Dynamic Adsorbents) were used to monitor the reactions, and spots were visualized by UV light. Flash column chromatography was performed by using silica gel (32–63 μm). All ^{1}H NMR, ^{13}C NMR, and ^{31}P NMR spectra were recorded with a Bruker 400 spectrometer. Chemical shift values are in ppm. ^{13}C NMR signals were determined by using the APT technique. High-resolution mass spectra were achieved by ESI at the University at Albany, SUNY.

Synthesis of cn^{5}U and cnm^{5}U phosphoramidites

1-(2′,3′,5′-Tri-*O*-acetyl-β-D-ribofuranosyl)-5-methyluridine (2):[22] 4-Dimethylaminopyridine (DMAP; 19 mg, 0.155 mmol) and Ac_2O (0.73 mL, 7.75 mmol) were added to a solution of compound **1** (200 mg, 0.77 mmol) in pyridine (8 mL) at room temperature. The mixture was stirred for 12 h. After the solvent had been removed, the residue was purified by silica gel column chromatography to give compound **2** (266 mg, 90%) as a light-brown oil. $R_f = 0.4$ (50% EtOAc/CH_2Cl_2); ^{1}H NMR (400 MHz, $CDCl_3$): $\delta = 7.18$ (s, 1H), 6.07 (d, $J = 4.8$ Hz, 1H), 5.33–5.30 (m, 2H), 4.36–4.33 (m, 3H), 2.17 (s, 3H), 2.13 (s, 3H), 2.10 (s, 3H), 1.95 ppm (s, 3H).

1-(2′,3′,5′-Tri-*O*-acetyl-β-D-ribofuranosyl)-5-bromomethyluridine (3):[23] NBS (90.31 mg, 0.51 mmol) and AIBN (8.33 mg, 0.05 mmol) were added to a solution of compound **2** (150 mg, 0.39 mmol) in benzene (4 mL). The mixture was heated at 80 °C for 4 h. After the solvent had been removed, the residue was purified by silica gel column chromatography to give compound **3** as a light-brown solid (140 mg, 80%). $R_f = 0.5$ (50% EtOAc/CH_2Cl_2). ^{1}H NMR (400 MHz, $CDCl_3$): $\delta = 7.65$ (s, 1H), 6.03 (d, $J = 4.8$ Hz, 1H), 5.39–5.27

(m, 2H), 4.42–4.22 (m, 5H), 2.17 (s, 3H), 2.12 (s, 3H), 2.09 ppm (s, 3H).

1-(2′,3′,5′-Tri-*O*-acetyl-β-D-ribofuranosyl)-5-cyanomethyluridine (4): TMSCN (0.24 mL, 1.95 mmol) and TBAF (1.95 mL, 1.95 mmol) were added to a solution of compound **3** (180.8 mg, 0.39 mmol) in THF (4 mL) at room temperature. The mixture was stirred for 1.5 h. The reaction was quenched with water, and the mixture was extracted with ethyl acetate. The organic layer was dried (Na_2SO_4), and the solvents were evaporated. The residue was purified by silica gel column chromatography to give compound **4** (111.8 mg, 70%) as a light-brown solid. R_f = 0.4 (50% EtOAc/CH_2Cl_2); ^{1}H NMR (400 MHz, $CDCl_3$): δ = 7.58 (s, 1H), 6.02–6.00 (m, 1H), 5.36–5.29 (m, 2H), 4.40–4.26 (m, 3H), 3.44 (s, 2H), 2.12 (s, 3H), 2.09 (s, 3H), 2.05 ppm (s, 3H); HRMS (ESI-TOF): *m/z* calcd for $C_{17}H_{19}N_3O_9 + Na^+$: 432.1121 $[M+Na]^+$; found: 432.1050.

5-Cyanomethyluridine (5):[18] A solution of ammonia (14:8 M, 0.19 mL, 2.93 mmol) was added to a solution of compound **4** (200 mg, 0.49 mmol) in MeOH (4 mL) at room temperature, and the resulting solution was stirred at room temperature for 15 h. The solvent was removed by repeat evaporation with the re-addition of MeOH to remove all ammonia. The residue was purified by silica gel column chromatography to give compound **5** (125 mg, 90%) as a white solid. R_f = 0.3 (20% MeOH/CH_2Cl_2); ^{1}H NMR (400 MHz, MeOD): δ = 8.16 (s, 1H), 5.90 (m, 1H), 4.17 (m, 2H), 4.02–3.99 (m, 1H), 3.89–3.83 (m, 1H), 3.77–3.74 (m, 1H), 3.48 ppm (s, 2H); HRMS (ESI-TOF): *m/z* calcd for $C_{11}H_{13}N_3O_6 + H^+$: 284.0883 $[M+H]^+$; found: 284.0868.

1-(5′-*O*-4,4′-Dimethoxytrityl-β-D-ribofuranosyl)-5-cyanomethyluridine (6): Compound **5** (200 mg, 0.706 mmol) evaporated with pyridine (3×) and was then dissolved in pyridine (7 mL). DMTrCl (286.99 mg, 0.847 mmol) was added. The mixture was stirred at room temperature in the dark for 12 h. The reaction was quenched with methanol (1 mL). The solvent was removed, and the residue was purified by silica gel column chromatography to give compound **6** (400 mg, 97%) as a white solid. R_f = 0.4 (10% MeOH/CH_2Cl_2); ^{1}H NMR (400 MHz, $CDCl_3$): δ = 7.98 (s, 1H), 7.39–7.37 (m, 2H), 7.34–7.25 (m, 7H), 6.87–6.84 (m, 4H), 5.96 (d, J = 3.2 Hz, 1H). 4.48–4.32 (m, 2H), 4.20–4.18 (m, 1H), 3.78 (s, 6H), 3.56–3.53 (m, 1H), 3.47–3.44 (m, 1H), 2.59 (d, J = 17.2 Hz, 1H), 2.46 ppm (d, J = 17.2 Hz, 1H); ^{13}C NMR (100 MHz, $CDCl_3$) δ = 162.4, 158.8, 158.8, 150.8, 144.2, 139.3, 135.1, 135.0, 130.1, 130.1, 128.2, 128.1, 127.4, 127.4, 113.4, 105.2, 87.2, 83.9, 55.2, 15.0 ppm; HRMS (ESI-TOF): *m/z* calcd for $C_{32}H_{31}N_3O_8 + Na^+$: 608.2009 $[M+Na]^+$; found: 608.2024.

1-(2′-*O*-*tert*-Butyldimethylsilyl-5′-*O*-4,4′-dimethoxytrityl-β-D-ribofuranosyl)-5-cyanomethyluridine (7): Pyridine (81 μL) and $AgNO_3$ (92.75 mg, 0.546 mmol) were added to a solution of compound **6** (200 mg, 0.342 mmol) in THF (3.5 mL). The mixture was stirred at room temperature in the dark for 30 min. Then, TBDMSCl (90.28 mg, 0.6 mmol) was added, and the resulting solution was stirred at room temperature in the dark for another 12 h. After the solvent had been removed, the residue was purified by silica gel column chromatography to give compound **7** (100 mg, 42%) as a white solid. R_f = 0.7 (5% MeOH/CH_2Cl_2); ^{1}H NMR (400 MHz, $CDCl_3$): δ = 7.98 (s, 1H), 7.39–7.25 (m, 9H), 6.89–6.86 (m, 4H), 6.0 (d, J = 3.2 Hz, 1H), 4.47–4.44 (m, 1H), 4.37–4.35 (m, 1H), 3.81 (s, 6H), 3.57–3.36 (m, 2H), 2.53 (d, J = 17.2 Hz, 1H), 2.28 (d, J = 17.2 Hz, 1H), 0.94 (s, 9H), 0.18 ppm (s, 6H); ^{13}C NMR (100 MHz, $CDCl_3$) δ = 159.0, 158.9, 149.8, 144.1, 138.7, 134.9, 134.7, 130.2, 130.1, 129.1, 128.1, 127.5, 116.1, 113.5, 113.3, 113.2, 105.3, 88.7, 87.3, 83.8, 62.8, 55.2, 25.6, 18.0, −4.7, −5.2 ppm; HRMS (ESI-TOF): *m/z* calcd for $C_{38}H_{45}N_3O_8Si + H^+$: 700.3054 $[M+H]^+$; found: 700.2960.

1-[2′-*O*-*tert*-Butyldimethylsilyl-3′-*O*-(2-cyanoethyl-*N*,*N*-diisopropylamino)phosphoramidite-5′-*O*-(4,4′-dimethoxytrityl-β-D-ribofuranosyl)]-5-cyanomethyluridine (8): *N*,*N*-Diisopropylethylamine (DIPEA; 0.14 mL, 0.8 mmol) was added to a solution of compound **7** (70 mg, 0.1 mmol) in THF (1 mL), and the mixture was stirred at room temperature for 30 min. $(i\text{Pr})_2\text{NPClOCH}_2\text{CH}_2\text{CN}$ (0.05 mL, 0.2 mmol) was added, and the mixture was stirred at room temperature for 12 h. The reaction was quenched with water, and the mixture was extracted with CH_2Cl_2. The organic layer was dried with anhydrous sodium sulfate, filtered, and concentrated under reduced pressure. The residue was purified by silica gel flash chromatography to give compound **8** (73 mg, 0.08 mmol, 80%) as a white solid. R_f = 0.7 (5% MeOH/CH_2Cl_2); ^{1}H NMR (400 MHz, $CDCl_3$): δ = 8.06–7.94 (m, 1H), 7.44–7.26 (m, 9H), 6.89–6.85 (m, 4H), 6.18–5.94 (m, 1H), 4.52–4.44 (m, 1H), 4.39–4.29 (m, 2H), 4.29–4.14 (m, 1H), 3.98–3.90 (m, 1H), 3.57–3.50 (m, 1H), 3.44–3.32 (m, 1H), 2.75–2.54 (m, 3H), 2.46–2.40 (m, 1H), 1.17 (s, 12H), 0.91 (s, 9H), 0.16 ppm (s, 6H); ^{31}P NMR (162 MHz, $CDCl_3$): δ = 149.89, 149.57 ppm; HRMS (ESI-TOF): *m/z* calcd for $C_{47}H_{62}N_5O_9PSi$: 900.4054 $[M+H]^+$: found: 900.4235.

1-(2′,3′,5′-Tri-*O*-benzoate-β-D-ribofuranosyl)-5-cyanouridine (11): TMSCl (15.2 mL, 120 mmol) was added to a solution of compound **9** (8.22 g, 60 mmol) in hexamethyldisilazane (HMDS, 500 mL). The mixture was stirred at 130 °C for 20 h until the mixture turned clear. Then, the solution was concentrated to remove the excess amount of HMDS, and compound **10** was obtained and immediately used without further purification. At room temperature, $SnCl_4$ (7.8 mL, 66 mmol) was added slowly to a solution of compound **10** and 2,3,5-tri-*O*-benzoyl-β-D-ribofuranose (33.26 g, 66 mmol) in 1,2-dichloroethane (DCE, 500 mL) at 0 °C. After 30 min, the mixture was brought to room temperature, and the reaction was continued for another 2 h. Then, the reaction was quenched with a saturated aqueous solution of $NaHCO_3$ (500 mL) at 0 °C, and the mixture was extracted with CH_2Cl_2 (3×500 mL). The organic layer was dried with anhydrous sodium sulfate, filtered, and concentrated under reduced pressure. The residue was purified by silica gel chromatography to give compound **11** (30 g, 51.64 mmol, 86%) as a white solid. R_f = 0.6 (10% MeOH/CH_2Cl_2); ^{1}H NMR (400 MHz, $CDCl_3$): δ = 8.14 (s, 1H), 8.10–7.88 (m, 6H), 7.64–7.33 (m, 9H), 6.23 (d, J = 5.2 Hz), 5.86 (m, 1H), 5.72–5.69 (m, 1H), 4.80 ppm (m, 3H); HRMS (ESI-TOF): *m/z* calcd for $C_{31}H_{23}N_3O_9 + NH_4^+$: 599.1778 $[M+NH_4]^+$; found: 599.1830.

5-Cyanouridine (12):[21] Compound **11** (5.81 g, 10 mmol) was dissolved in 7 N NH_3/MeOH (50 mL) at room temperature, and the mixture was stirred for 12 h. The solvent was removed by repeat evaporation with the re-addition of MeOH to remove all ammonia. The residue was purified by silica gel chromatography to give compound **12** (1.80 g, 6.69 mmol, 67%) as a white solid. R_f = 0.4 (25% MeOH/CH_2Cl_2); ^{1}H NMR (400 MHz, MeOD): δ = 9.02 (s, 1H), 5.83 (d, J = 2.8 Hz, 1H), 4.21–4.16 (m, 2H), 4.07–4.03 (m, 1H), 3.95 (dd, J = 2.4 Hz, 12.4 Hz, 1H), 3.77 ppm (dd, J = 2.4 Hz, 12.4 Hz, 1H); HRMS (ESI-TOF): *m/z* calcd for $C_{10}H_{11}N_3O_6 + Na^+$: 292.0546 $[M+Na]^+$; found: 292.0564.

1-(2′-*O*-*tert*-Butyldimethylsilyl-3′,5′-*O*-di-*tert*-butylsilylene-β-D-ribofuranosyl)-5-cyanouridine (13): Compound **12** (1.40 g, 5.2 mmol) was suspended in DMF (20 mL) and cooled to 0 °C. Then, di-*tert*-butylsilyl bis(trifluoromethanesulfonate) (2.4 mL, 6.24 mmol) was added dropwise, and the resulting solution was stirred at 0 °C for 1 h. Subsequently, imidazole (2.04 g, 26 mmol) was added, and the mixture was warmed to room temperature, at which point TBDMSCl (1.1 g, 6.24 mmol) was added. The reaction was allowed to proceed at 60 °C for 2 h. Then, the reaction was

quenched with water (50 mL), and the mixture was extracted with CH_2Cl_2 (3×50 mL). The organic layer was dried with anhydrous sodium sulfate, filtered, and concentrated under reduced pressure. The residue was purified by silica gel chromatography to give compound **13** (2.40 g, 4.59 mmol, 88%) as a white solid. $R_f = 0.7$ (30% EtOAc/hexane); ^{1}H NMR (400 MHz, $CDCl_3$): $\delta = 7.91$ (s, 1H), 5.64 (s, 1H), 4.58–4.53 (m, 1H), 4.30–4.23 (m, 2H), 4.03–3.98 (m, 1H), 3.78–3.73 (m, 1H), 1.06 (s, 9H), 1.03 (s, 9H), 0.94 (s, 9H), 0.19 (s, 3H), 0.15 ppm (s, 3H); ^{13}C NMR (100 MHz, $CDCl_3$): $\delta = 159.52$, 159.47, 148.2, 147.5, 112.8, 94.1, 90.1, 75.3, 75.1, 22.6, 20.3, 18.1, −4.1, −4.3, −5.0, −5.2 ppm; HRMS (ESI-TOF): *m/z* calcd for $C_{24}H_{41}N_3O_6Si_2 + H^+$: 524.2612 $[M+H]^+$; found: 524.2641.

1-(2′-*O*-*tert*-Butyldimethylsilyl-β-D-ribofuranosyl)-5-cyanouridine (14): A solution of HF·Py (hydrogen fluoride ≈70%, pyridine ≈30%, 0.4 mL) in pyridine (2 mL) was added to a solution of compound **13** (2.10 g, 4.00 mmol) in THF (20 mL) at 0 °C. After 1 h at 0 °C, the reaction was complete, and pyridine (15 mL) was added. The mixture was washed with saturated $NaHCO_3$, dried with Na_2SO_4, and concentrated. The residue was purified by silica gel chromatography to give compound **14** (1.10 g, 2.87 mmol, 75%) as a white solid. $R_f = 0.4$ (10% MeOH/CH_2Cl_2); ^{1}H NMR (400 MHz, CD_3OD): $\delta = 9.12$ (s, 1H), 5.76 (s, 1H), 4.27 (m, 1H), 4.15–4.04 (m, 2H), 4.01–3.97 (m, 1H), 3.81–3.77 (m, 1H), 0.94 (s, 9H), 0.15 ppm (d, 6H); ^{13}C NMR (100 MHz, $CDCl_3$): $\delta = 160.61$, 160.60, 149.7, 149, 4, 149, 1, 113.2, 90.8, 88.3, 76.7, 76.4, 17.6, −6.0 ppm; HRMS (ESI-TOF): *m/z* calcd for $C_{16}H_{25}N_3O_6Si + Na^+$: 406.1410 $[M+Na]^+$; found: 406.1411.

1-(2′-*O*-*tert*-Butyldimethylsilyl-5′-*O*-4,4′-dimethoxytrityl-β-D-ribofuranosyl)-5-cyanouridine (15): 4,4′-Dimethoxytrityl chloride (812 mg, 2.4 mmol) was added to a solution of compound **14** (766 mg, 2 mmol) in dry pyridine (10 mL) under an argon atmosphere. The resulting solution was stirred at room temperature for 12 h. The reaction was quenched with methanol (1 mL), and the mixture was stirred for another 5 min. The mixture was then concentrated to dryness under vacuum. The residue was purified by silica gel chromatography to give compound **15** (1.20 g, 1.75 mmol, 73%) as a white solid. $R_f = 0.5$ (50% EtOAc/hexane); ^{1}H NMR (400 MHz, $CDCl_3$): $\delta = 8.42$ (s, 1H), 7.42–7.39 (m, 2H), 7.35–7.24 (m, 7H), 6.89–6.86 (m, 4H), 5.90 (d, $J = 3.2$ Hz, 1H), 4.50 (m, 1H), 4.43 (m, 1H), 4.22 (m, 1H), 3.80 (s, 6H), 3.58–3.55 (m, 1H), 3.42–3.35 (m, 1H), 0.95 (s, 9H), 0.19 ppm (d, 6H); ^{13}C NMR (100 MHz, $CDCl_3$): $\delta = 159.1$, 158.8, 158.7, 148.6, 147,8, 147.68, 147,67, 144.0, 135.1, 134.7, 113.6, 113.4, 111.6, 90.8, 89.8, 89.76, 87.4, 80.3, 70.7, 18.0, −4.6, −5.1 ppm; HRMS (ESI-TOF): *m/z* calcd for $C_{37}H_{43}N_3O_8Si + Na^+$: 708.2717 $[M+Na]^+$; found: 708.2716.

1-[2′-*O*-*tert*-Butyldimethylsilyl-3′-*O*-(2-cyanoethyl-*N*,*N*-diisopropylamino)phosphoramidite-5′-*O*-(4,4′-dimethoxytrityl-β-D-ribofuranosyl)]-5-cyanouridine (16): DIPEA (0.7 mL) and 2-cyanoethyl *N*,*N*-diisopropylchlorophosphoramidite (0.5 mL) were added to a solution of compound **15** (685 mg, 1 mmol) in dry THF (8 mL). The resulting solution was stirred at room temperature for 12 h under an argon atmosphere. The reaction was quenched with water, and the mixture was extracted with ethyl acetate. The organic layer was dried (Na_2SO_4) and concentrated. The residue was purified by silica gel flash chromatography to give compound **16** (800 mg, 0.9 mmol, 90%) as a white solid. $R_f = 0.5$ (50% EtOAc/hexane); ^{1}H NMR (400 MHz, $CDCl_3$): $\delta = 8.43$–8.38 (m, 1H), 7.49–7.25 (m, 9H), 6.90–6.87 (m, 4H), 5.92–5.77 (m, 1H), 4.61 (m, 1H), 4.44–4.33 (m, 2H), 3.80 (s, 6H), 3.63–3.46 (m, 5H), 2.69–2.65 (m, 1H), 2.47 (m, 1H), 1.17 (s, 12H), 0.92 (s, 9H), 0.18 ppm (s, 6H); ^{31}P NMR (162 MHz, $CDCl_3$): $\delta = 150.09$, 149.63 ppm; HRMS (ESI-TOF): *m/z* calcd for $C_{46}H_{60}N_5O_9PSi + H^+$: 886.3976 $[M+H]^+$; found: 886.4015.

Synthesis, HPLC, and characterization of RNA oligonucleotides: All oligonucleotides were chemically synthesized at a 1.0 μmol scale by solid-phase synthesis by using the Oligo-800 synthesizer. The cnm^{5}U and cn^{5}U phosphoramidites were dissolved in acetonitrile to a concentration of 0.07 M. I_2 (0.02 M) in THF/Py/H_2O solution was used as an oxidizing reagent. Coupling was performed by using 5-ethylthio-1*H*-tetrazole solution (0.25 M) in acetonitrile for 12 min for both the native and modified phosphoramidites. About 3% trichloroacetic acid in methylene chloride was used for 5′-detritylation. Synthesis was performed on control-pore glass (CPG-500) immobilized with the appropriate nucleoside through a succinate linker. All the reagents used were standard solutions obtained from ChemGenes Corporation. All canonical rA, U, rG, and rC phosphoramidites were purchased from ChemGenes Corporation. Phosphoramidite rA was *N*-Bz protected, rC was *N*-Ac protected, and rG was *N*-*i*Bu protected. The oligonucleotide was prepared in DMTr off form. After synthesis, the oligonucleotides were cleaved from the solid support and were fully deprotected with concentrated ammonium solution at room temperature for 14 h. The solution was evaporated to dryness by using a Speed-Vac concentrator. The solid was dissolved in DMSO (100 μL) and was desilylated by using a solution of $Et_3N{\cdot}3HF$ at 65 °C for 2.5 h. Cooled down to room temperature, the RNA was precipitated by adding 3 M sodium acetate (0.025 mL) and ethanol (1 mL). The solution was cooled to −80 °C for 1 h before the RNA was recovered by centrifugation and finally dried under vacuum.

The oligonucleotides were purified by reverse-phase HPLC on a Zorbax SB-C_{18} column at a flow rate of 1 mL min^{-1}. Buffer A was 20 mM Tris·HCl, pH 8.0; buffer B was 1.25 M NaCl in 20 mM Tris·HCl, pH 8.0. A linear gradient from 100% buffer A to 70% buffer B in 20 min was used to elute the oligonucleotides. Analysis was performed by using the same type of analytical column with the same eluent gradient. All the modified oligonucleotides were checked by high-resolution MS.

UV-melting temperature (T_m) study: Solutions of the duplex RNAs (1.5 μM) were prepared by dissolving the purified RNAs in sodium phosphate (10 mM, pH 7.0) buffer containing 100 mM NaCl. The solutions were heated to 95 °C for 5 min, then cooled down slowly to room temperature, and stored at 4 °C for 2 h before the T_m measurements. Thermal denaturation was performed in a Cary 300 UV/Vis Spectrophotometer with a temperature controller. The temperature reported is the block temperature. Each denaturizing curve was acquired at $\lambda = 260$ nm by heating and cooling from 5 to 80 °C (4×) at a rate of 0.5 °C min^{-1}. All the melting curves were repeated at least four times. The thermodynamic parameter of each strand was obtained by fitting the melting curves in the Meltwin software.

Simulation method: We performed molecular dynamics (MD) simulations of the RNA duplex in the presence and absence of the modification. To do so, we developed AMBER-type[24] force-field parameters for the modified uridine in the following way. We performed restrained electrostatic potential (RESP) fit on the RED server[25] at the Hartree–Fock (HF) level of theory with the 6-31G* basis set to obtain partial charges of the modified base.[26] The bonded interactions were obtained from General AMBER Force-field (GAFF), and the nonbonded interactions were obtained from AMBER99 force-field with Chen-Garcia corrections.[27] The rest of the duplex also employed AMBER99 force-filed with Chen-Garcia corrections for the base and Cheatham–Bergonzo[28] corrections for the backbone atoms.

The duplex was constructed as an A-form helix by using the makena server by employing the NAB suite of AMBER. The modification was introduced in the duplex and was minimized under vacuum before it was introduced in the 0.1 M NaCl solution. The simulation system was a $6\times6\times6$ nm^3 3D periodic box containing the RNA duplex, 6763 water molecules, 35 Na^+ ions, and 13 Cl^- ions. The TIP4P-Ew[29] model was used for the water molecules, and Joung and Cheatham parameters[30] were used for the ions.

All simulations were performed by using the Gromacs-2016 simulation package. The simulations incorporated a leap-frog algorithm with a time step of 1 fs. The systems were studied in the NPT ensemble by maintaining the temperature at 300 K and the pressure at 1 bar by using a V-rescale thermostat[31] and Parrinello–Rahman,[32] respectively. The electrostatic interactions were calculated by using Particle Mesh Ewald (PME)[33] with a real space cut off of 1.2 nm. LJ interactions were also cut off at 1.2 nm. LINCS algorithm[34] was used to constrain H-bonds. The production runs consisted of ten 100 ns runs starting from an equilibrated system for a total of a microsecond of data to analyze for each of the duplexes. The configurations of the RNA were stored at 2 ps intervals for further analysis.

Acknowledgements

We are grateful to the National Science Foundation (NSF; MCB-1715234) and the University at Albany, State University of New York, for financial support. We thank Prof. Maksim Royzen, Prof. Daniele Fabris, Dr. Reza Nemti, Cen Chen, Muhan He, and Thomas Kenderdine for their help with MS analysis.

Conflict of Interest

The authors declare no conflict of interest.

Keywords: base pairs · oligonucleotides · phosphoramidites · RNA · solid-phase synthesis

[1] M. J. Fedor, *Annu. Rev. Biophys.* **2009**, *38*, 271 – 299.
[2] J. A. Doudna, J. R. Lorsch, *Nat. Struct. Mol. Biol.* **2005**, *12*, 395 – 402.
[3] T. M. Henkin, *Gene. Dev.* **2008**, *22*, 3383 – 3390.
[4] A. Roth, R. R. Breaker, *Annu. Rev. Biochem.* **2009**, *78*, 305 – 334.
[5] P. Boccaletto, M. A. Machnicka, E. Purta, P. Piatkowski, B. Baginski, T. K. Wirecki, V. de Crécy-Lagard, R. Ross, P. A. Limbach, A. Kotter, M. Helm, J. M. Bujnicki, *Nucleic Acids Res.* **2018**, *46*, D303 – D307.
[6] W. A. Cantara, P. F. Crain, J. Rozenski, J. A. McCloskey, K. A. Harris, X. Zhang, F. A. Vendeix, D. Fabris, P. F. Agris, *Nucleic Acids Res.* **2011**, *39*, D195 – D201.
[7] C. J. Lewis, T. Pan, A. Kalsotra, *Nat. Rev. Mol. Cell Biol.* **2017**, *18*, 202 – 210.
[8] N. B. Leontis, J. Stombaugh, E. Westhof, *Nucleic Acids Res.* **2002**, *30*, 3497 – 3531.
[9] P. H. Hagedorn, B. R. Hansen, T. Koch, M. Lindow, *Nucleic Acids Res.* **2017**, *45*, 2262 – 2282.
[10] H. Grosjean, *DNA and RNA Modification Enzymes: Structure, Mechanism, Function and Evolution*, Landes Bioscience, Austin, **2009**, pp. 1 – 18.
[11] P. F. Agris, F. A. Vendeix, W. D. Graham, *J. Mol. Biol.* **2007**, *366*, 1 – 13.
[12] S. Yokoyama, S. Nishimura, *tRNA: Structure, Biosynthesis, and Function*, American Society for Microbiology, Washington, D.C., **1995**, pp. 207 – 224.
[13] G. R. Björk, *tRNA: Structure, Biosynthesis, and Function*, American Society for Microbiology, Washington, D.C., **1995**, pp. 165 – 205.
[14] T. Suzuki, *Top. Curr. Genet.* **2005**, *12*, 23 – 69.
[15] M. Helm, J. D. Alfonzo, *Chem. Biol.* **2014**, *21*, 174 – 185.
[16] D. Mandal, C. Köhrer, D. Su, I. R. Babu, C. T. Y. Chan, Y. Liu, D. Söll, P. Blum, M. Kuwahara, P. C. Dedon, U. L. Rajbhandary, *RNA* **2014**, *20*, 177 – 188.
[17] M. Egli, P. S. Pallan, *Annu. Rev. Biophys. Biomol. Struct.* **2007**, *36*, 281 – 305.
[18] K. Bartosik, E. Sochacka, G. Leszczynska, *Org. Biomol. Chem.* **2017**, *15*, 2097 – 2103.
[19] G. T. Badman, C. B. Reese, *J. Chem. Soc. Chem. Commun.* **1987**, 1732 – 1734.
[20] K. Ikeda, S. Tanaka, Y. Mizuno, *Chem. Pharm. Bull.* **1975**, *23*, 2958 – 2964.
[21] M. E. Meza-Avina, L. Wei, Y. Liu, E. Poduch, A. M. Bello, R. K. Mishra, E. F. Pai, L. P. Kotra, *Bioorg. Med. Chem.* **2010**, *18*, 4032 – 4041.
[22] K. Takenuki, H. Itoh, A. Matsuda, T. Ueda, *Chem. Pharm. Bull.* **1990**, *38*, 2947 – 2952.
[23] M. Münzel, D. Globisch, T. Bruckl, M. Wagner, V. Welzmiller, S. Michalakis, M. Müller, M. Biel, T. Carell, *Angew. Chem. Int. Ed.* **2010**, *49*, 5375 – 5377; *Angew. Chem.* **2010**, *122*, 5503 – 5505.
[24] W. D. Cornell, P. Cieplak, C. I. Bayly, I. R. Gould, K. M. Merz, D. M. Ferguson, D. C. Spellmeyer, T. Fox, J. W. Caldwell, P. A. Kollman, *J. Am. Chem. Soc.* **1995**, *117*, 5179 – 5197.
[25] F. Y. Dupradeau, A. Pigache, T. Zaffran, C. Savineau, R. Lelong, N. Grivel, D. Lelong, W. Rosanski, P. Cieplak, *Phys. Chem. Chem. Phys.* **2010**, *12*, 7821 – 7839.
[26] W. D. Cornell, P. Cieplak, C. I. Bayly, P. A. Kollman, *J. Am. Chem. Soc.* **1993**, *115*, 9620 – 9631.
[27] A. A. Chen, A. E. García, *Proc. Natl. Acad. Sci. USA* **2013**, *110*, 16820 – 16825.
[28] C. Bergonzo, T. E. Cheatham III, *J. Chem. Theory Comput.* **2015**, *11*, 3969 – 3972.
[29] C. Vega, J. L. Abascal, I. Nezbeda, *J. Chem. Phys.* **2006**, *125*, 34503.
[30] I. S. Joung, T. E. Cheatham III, *J. Phys. Chem. B* **2008**, *112*, 9020 – 9041.
[31] G. Bussi, D. Donadio, M. Parrinello, *J. Chem. Phys.* **2007**, *126*, 014101.
[32] H. J. C. Berendsen, J. P. M. Postma, W. F. van Gunsteren, A. DiNola, J. R. Haak, *J. Chem. Phys.* **1984**, *81*, 3684 – 3690.
[33] T. A. Darden, L. G. Pedersen, *Environ. Health Perspect.* **1993**, *101*, 410 – 412.
[34] B. Hess, B. Bekker, H. J. C. Berendsen, J. G. E. M. Fraaije, *J. Comput. Chem.* **1997**, *18*, 1463 – 1472.
[35] J. A. McDowell, D. H. Turner, *Biochemistry* **1996**, *35*, 14077 – 14089.

Manuscript received: July 17, 2018
Revised manuscript received: September 21, 2018
Accepted manuscript online: October 7, 2018
Version of record online: November 19, 2018